Energy Conversion and Management: X 31 (2026) 101940

Contents lists available at ScienceDirect

Energy Conversion and Management: X

journal homepage: www.sciencedirect.com/journal/energy-conversion-and-management-x

Thermal hardware-in-the-loop: concept, implementation, and experimental validation

Nima Ghorbani [a,*], Fargah Ashrafidehkordi [a], Veit Hagenmeyer [b], Giovanni De Carne [a]

[a] Institute for Technical Physics (ITEP), Karlsruhe Institute of Technology, 76344, Karlsruhe, Germany
[b] Institute for Automation and Applied Informatics (IAI), Karlsruhe Institute of Technology, 76344, Karlsruhe, Germany

ARTICLE INFO

Keywords:
Thermal hardware-in-the-loop
Real-time simulation
Power hardware-in-the-loop
Interface algorithm
Thermal interface
Space heating

ABSTRACT

As energy systems become more integrated, thermal equipment, alongside electrical equipment, plays a significant role in future energy grids. Therefore, there is a critical need for experimental platforms that allow flexible and accurate evaluation of thermal technologies. This paper presents a thermal hardware-in-the-loop (THIL) concept to provide a reliable framework for testing thermal sources and loads. THIL modeling of two case studies is implemented in MATLAB/Simulink and validated experimentally using a 15.6 kW heat exchanger and the OPAL-RT real-time simulator. In the THIL setup, a space heating load model is compiled on the real-time simulator and connected to an electric water heater via a heat exchanger, which serves as the thermal interface. The real-time simulation sends the heat exchanger fan speed as a forward path to the setup and receives the measured hot water supply temperature and flow rate as feedback. In both case studies, a step change in ambient temperature is considered in the load model to evaluate THIL response to a sudden and substantial change in thermal load, while in the first case, the flow rate in the space heating circuit is constant, and in the second case, it varies with the ambient temperature changes. Measurement uncertainties are calculated to support the reliability of the experimental results.

1. Introduction

Testing products either as software models during primary design or as real hardware prior to final production plays an essential role across various industries. For example, in the energy industry, before releasing a product such as a gas turbine, fuel cell, or converter to the market, numerous tests are conducted based on its intended use to ensure its proper performance and reliability under operating conditions. Since the 1970s, various test methods have been developed to evaluate equipment performance and control algorithms [1,2]. A purely software-based testing approach, e.g., Model-in-the-Loop (MIL), enables closed-loop evaluation of a device model interacting with a simulated plant model, mostly employed during the early stages of device design and development [1,3]. On the other hand, hybrid environments such as Hardware-in-the-Loop (HIL) [4] integrate both hardware and software components, which provides validity of experimental tests in realistic conditions, in addition to software flexibility.

As various scenarios for energy production and consumption are being introduced, testing equipment used in the energy grid, as well as evaluating different solutions to supply and distribute energy, are becoming more essential. Such assessments can contribute significantly to optimizing energy production and consumption over time. Therefore, a realistic test environment is necessary in which the product can be tested in various ways without risking damage to either the product itself or the energy grid. A particular configuration of HIL, known as Power Hardware-in-the-Loop (PHIL), consists of Hardware-of-Interest (HoI), Model-of-Interest (MoI), and an interface [5] has been introduced for testing electrical systems prior to deployment in the grid [6,7]. PHIL provides a reliable and cost-effective test of electrical hardware connected to a simulated electrical grid running on a digital real-time simulator (DRTS) via a power amplifier [8]. However, its applications remain limited to the electrical systems [9].

Energy systems are becoming increasingly integrated, and thermal systems play a crucial role alongside electrical systems in modern energy grids [10]. In the European Union (EU), buildings account for approximately 40% of final energy consumption, of which about 80% is for space heating and domestic hot water (DHW) [11]. Several studies have examined the load-flexibility potential of thermal systems, including residential thermal energy storage [12], modulating Heating, Ventilation, and Air Conditioning (HVAC) systems with price-based or occupant-based control [11,13], and model predictive control (MPC)

* Corresponding author.
E-mail addresses: nima.ghorbani@kit.edu (N. Ghorbani), fargah.ashrafidehkordi@kit.edu (F. Ashrafidehkordi), veit.hagenmeyer@kit.edu (V. Hagenmeyer), giovanni.carne@kit.edu (G. De Carne).

https://doi.org/10.1016/j.ecmx.2026.101940
Received 27 March 2026; Received in revised form 2 May 2026; Accepted 8 May 2026
Available online 18 May 2026

Nomenclature

C_P	Specific heat of water (J/(kgK))
$\dot{m}_{HoI}$	Hot water mass flow rate in the HoI (kg/s)
$\dot{m}^*_{HoI}$	Setpoint hot water mass flow rate (kg/s)
$\dot{m}_{MoI}$	Hot water mass flow rate in the MoI (kg/s)
$\dot{Q}_{HoI}$	Thermal load in the HoI (W)
$\dot{Q}_{MoI}$	Thermal load in the MoI (W)
$T_{s,HoI}$	Hot water supply temperature in the HoI (K)
$T_{r,HoI}$	Hot water return temperature in the HoI (K)
$T_{s,MoI}$	Hot water supply temperature in the MoI (K)
$T_{r,MoI}$	Hot water return temperature in the MoI (K)
ΔT_{HoI}	Temperature difference in the HoI (K)
ΔT_{MoI}	Temperature difference in the MoI (K)

Greek Symbols

ω	Fan speed (rpm)

Subscripts and Abbreviations

s	Supply
r	Return
DRTS	Digital Real-time Simulator
HWST	Hot water supply temperature
HWRT	Hot water return temperature
HoI	Hardware of Interest
MoI	Model of Interest
PHIL	Power Hardware-in-the-Loop
THIL	Thermal Hardware-in-the-Loop

approaches for district heating networks (DHNs) [14] to mitigate grid load during peak hours. The significance of thermal systems in the energy grid highlights the need to develop realistic test benches for evaluating these systems and their control strategies.

Over the past decade, efforts have been made to develop HIL test benches for thermal systems, including vehicle thermal management systems [15], HVAC systems [16], and CHP units [17], primarily employing an emulator unit as an interface between the simulated model and the hardware. More recent studies have further extended HIL-based testing of thermal systems, particularly for heat pumps. The impact of thermal storage on the exergy losses of a ground-source heat pump is investigated in [18]. Researchers in [19] developed a dedicated testbed to evaluate the performance of a water-source heat pump. In [20], the demand flexibility of a prototype Phase Change Material-coupled ground-source heat pump is assessed. Moreover, HIL-based analysis of district heating and cooling (DHC) networks has also been investigated in recent years. The work in [21] introduces a laboratory for testing DHC networks with a case study on the flexible operation of prosumer-based DHC systems. A new hydraulic design and two control strategies are tested for a 5th generation DHC network in [22]. Furthermore, the analysis of strategies to improve energy self-consumption of prosumers in DHN is addressed in [23] using the HIL method. However, these studies rarely focus on establishing a generalized HIL framework for thermal systems with a structured interface algorithm and validating its accuracy in reproducing the modeled thermal load. Furthermore, they predominantly rely on National Instruments (NI) and LabVIEW, requiring complex communication interfaces rather than a dedicated digital real-time simulator as the core execution and data-acquisition platform.

To bridge this gap, the present article proposes a digital real-time simulator (DRTS)-based Thermal Hardware-in-the-Loop (THIL) concept with clearly defined THIL components and a feasible interface algorithm. The concept is developed in MATLAB/Simulink and validated experimentally. The main contributions of the present work can be summarized as follows:

- Introducing a DRTS-based THIL framework for testing dynamic thermal loads and sources, which provides the advantage of executing complex models and facilitates the integration of THIL into a multi-physics HIL framework in the future.
- Proposing a structured interface algorithm, including PI controller-based load tracking, for accurate closed-loop interaction between the simulated model and the hardware.
- Experimental validation of the proposed THIL arrangement through two representative case studies, considering THIL accuracy in tracking fast dynamics.

This paper is structured as follows: Section 2 reviews the related work in hardware-in-the-loop testing for thermal equipment. Section 3 introduces the Thermal Hardware-in-the-Loop concept. The interface algorithm for creating a Thermal Hardware-in-the-Loop is proposed in Section 4. In Section 5, software modeling is presented, and simulation results are discussed in terms of thermal load, working fluid temperature, room temperature, and fan speed. In Section 6, the THIL setup is introduced, and experimental results have been provided to validate the recommended THIL arrangement. Finally, the key findings of this research are summarized in Section 7.

2. Related work

This section provides an overview of key studies that employed the Hardware-in-the-Loop approach to test thermal equipment, discusses their findings, and addresses research gaps in this area. One of the first efforts to establish an HIL setup specifically dedicated to testing a thermal-fluid system is presented in [24]. A test bench was developed to evaluate the thermal management system of a plug-in hybrid electric vehicle. In that work, the vehicle's thermal load was modeled in Dymola, while the actual thermal management system served as the HoI. Interaction between the simulated environment and the physical system was implemented using LabVIEW and VeriStand, integrated with CompactRIO hardware. A control strategy for the same experimental setup was developed to regulate the HoI desired inlet temperature and flow rate [25]. In another study on vehicle thermal management systems, an HIL test bench was developed to evaluate the heating system of conventional coaches [15]. A dynamic cabin thermal model, including driver and passenger compartments, was implemented in MATLAB/Simulink, while the real HVAC unit of a coach served as the HoI. To emulate the engine cooling circuit, a water boiler coupled to a buffer tank supplied hot water to the HVAC unit, with control valves adjusting both flow rate and temperature of the hot water. An external refrigeration unit reproduced ambient air conditions at the heat exchanger inlet. Real-time bidirectional communication was established via OPC UA over a programmable logic controller (PLC) and LabVIEW. The Simulink controller sent hot water valve position and fan Pulse Width Modulation (PWM) commands to the PLC to regulate the air supply temperature and air mass flow rate. In return, the PLC fed back the measured air supply temperature and air mass flow rate to the model.

Due to the significance of residential thermal loads in smart energy grids, most studies have focused on this area, evaluating equipment performance and control strategies. Researchers in [26] conducted an HIL evaluation of a ground-source heat pump, an air-source heat pump, and a micro combined heat and power system (mCHP) performance. The heat source was coupled to a DHW tank and a buffer storage tank to supply both the DHW and space heating loads, while a hydraulic test bench emulated the building's thermal power demand. The building thermal load was modeled in TRNSYS and Dymola, which receives the measured hot water supply temperature and flow rate from the hardware and sends the calculated hot water return temperature and flow rate, as setpoints, as well as DHW consumption, to the hydraulic test bench in real time. Similarly, thermal load of a single-family house was simulated to evaluate the performance of a heat pump

Table 1
Summary of state-of-the-art on HIL testing of thermal systems.

Reference	Main focus	Real-time simulation	Dedicated DRTS[a]	Single sub-second time step	Rapid dynamics analysis	Load-tracking analysis
[16]	HIL testbed for optimization of heating system control	✓	✗	NA[b]	✗	✗
[26]	ASHP[c], GSHP[d], and mCHP annual efficiency assessment	✓	✗	✗	✗	✗
[28]	ASHP performance assessment	NA	✗	NA	✗	✗
[17]	Optimization of mCHP control algorithm	✗	✗	✗	✗	✗
[19]	HIL testbed for WSHP[e] performance assessment	✓	✗	✗	✗	✓
[21]	HIL laboratory architecture for sector-coupled DHC systems	✓	✗	✗	✗	✓
[29]	HIL testbed for ASHP control and energy flexibility assessment	✓	✗	✗	✗	✓
[23]	Prosumer's energy self-consumption in DHN	✓	✗	✗	✗	✗
This paper	DRTS-based THIL framework for thermal systems testing	✓	✓	✓	✓	✓

[a] Dedicated DRTS: Specialized real-time simulator used to run the load model and manage bidirectional communication.
[b] NA: Not Available.
[c] ASHP: Air-Source Heat Pump.
[d] GSHP: Ground-Source Heat Pump.
[e] WSHP: Water-Source Heat Pump.

integrated with a photovoltaic thermal (PVT) collector, using an HIL approach [27]. The space heating load was simulated in TRNSYS, while a predefined tapping profile was employed to represent DHW consumption. On the demand side, the heat pump was connected to a thermal storage tank that supplied DHW and hot water to a heat exchanger, which emulated the space heating load. System control and real-time communication between the simulation model and physical hardware were implemented via LabVIEW. The model received the hot water supply temperature from the hardware and returned the hot water return temperature and mass flow rate.

The performance of an air-source heat pump for space heating during winter was evaluated using an HIL setup in [28]. A thermal storage tank was integrated as a backup to support the heat pump to meet the required thermal demand, while the building load was emulated using an air-water heat exchanger. The heat pump and the load emulator are thermally coupled via an intermediate heat exchanger rather than connected directly. A dynamic building model was simulated in MATLAB, and the HIL setup, including simulation control and data acquisition, was managed every minute using LabVIEW virtual instruments (VIs). A proportional–integral–derivative (PID) controller regulated a three-way mixing valve between the air-water heat exchanger inlet and outlet to adjust the water return temperature, ensuring that the emulator delivered the power computed by the building model. In parallel, a thermostat controlled the heat pump's operation based on the simulated indoor temperature. The same HIL setup was utilized to validate a heat pump model to analyze the effects of coupling the heat pump with a thermal storage unit on its performance [30].

As previously discussed, the HIL approach can be used not only to evaluate equipment performance and reliability but also to modify control strategies for energy systems and to validate simulated models. An HIL test bench was developed to assess the performance of the HVAC system and optimize its control strategies in [16]. In their study, an air-source heat pump was employed as the heat source to meet both space heating and DHW demands, although not simultaneously. A DHW storage tank was coupled to the heat pump to supply hot water, while a hot tap water unit was connected to the tank to emulate DHW consumption based on a real tapping profile. For space heating, a cooling water unit was used to emulate the thermal load of a building model simulated in Dymola. Real-time communication between the simulation model and the physical components was established via an OPC (OLE – Object Linking and Embedding – for Process Control) server and LabVIEW. The hardware provided the model with the hot water supply temperature and mass flow rate, while the model returned the hot water return temperature as a control reference for the cooling water unit. Ambient temperature and solar radiation were also measured and transmitted to the model. A thermostat model, receiving indoor temperature from the building simulation, generated on/off control signals for the heat pump based on the desired setpoint temperature. In another research [17], an HIL approach was used to test and optimize a control algorithm for a CHP unit in combination with thermal energy storage. The optimization algorithm was executed in MATLAB and interfaced with the hardware through LabVIEW, which served as the data acquisition and communication platform. The thermal energy storage unit was coupled to a DHW station and a space heating emulator driven by pre-recorded load profiles of single-family houses. The results showed that, compared to conventional heat-led control strategies, a demand-oriented control algorithm can enhance the on-site utilization of CHP-generated electricity, thereby reducing consumer costs and relieving the load on the power grid. They declared that the HIL approach provides an effective, practical, and automated framework for testing and optimizing predictive control algorithms for CHP systems integrated with thermal energy storage.

More recently, a heat pump digital twin and its control strategies were validated with HIL in [31]. The HIL test bench consisted of an air-source heat pump as the heat source, with its indoor unit connected to a buffer tank coupled to a heat sink to simulate the space heating load of a building. The thermal load of a building was modeled in Dymola and communicated with the hardware in real time through LabVIEW. The hot water supply temperature and flow rate were sent to the model, and the hardware received the hot water return temperature and flow rate as setpoints. Researchers in [29] developed an HIL testbed for evaluating heat pump energy flexibility. The building's thermal load, including both space heating and DHW demand, was simulated using TRNSYS. In the physical testbed, separate emulators were used to represent the dynamic thermal demand for space heating and DHW. The heat pump was connected to a thermal storage tank that supplied hot water to both emulators, replicating real building operation. A custom-developed middleware was used for communication between

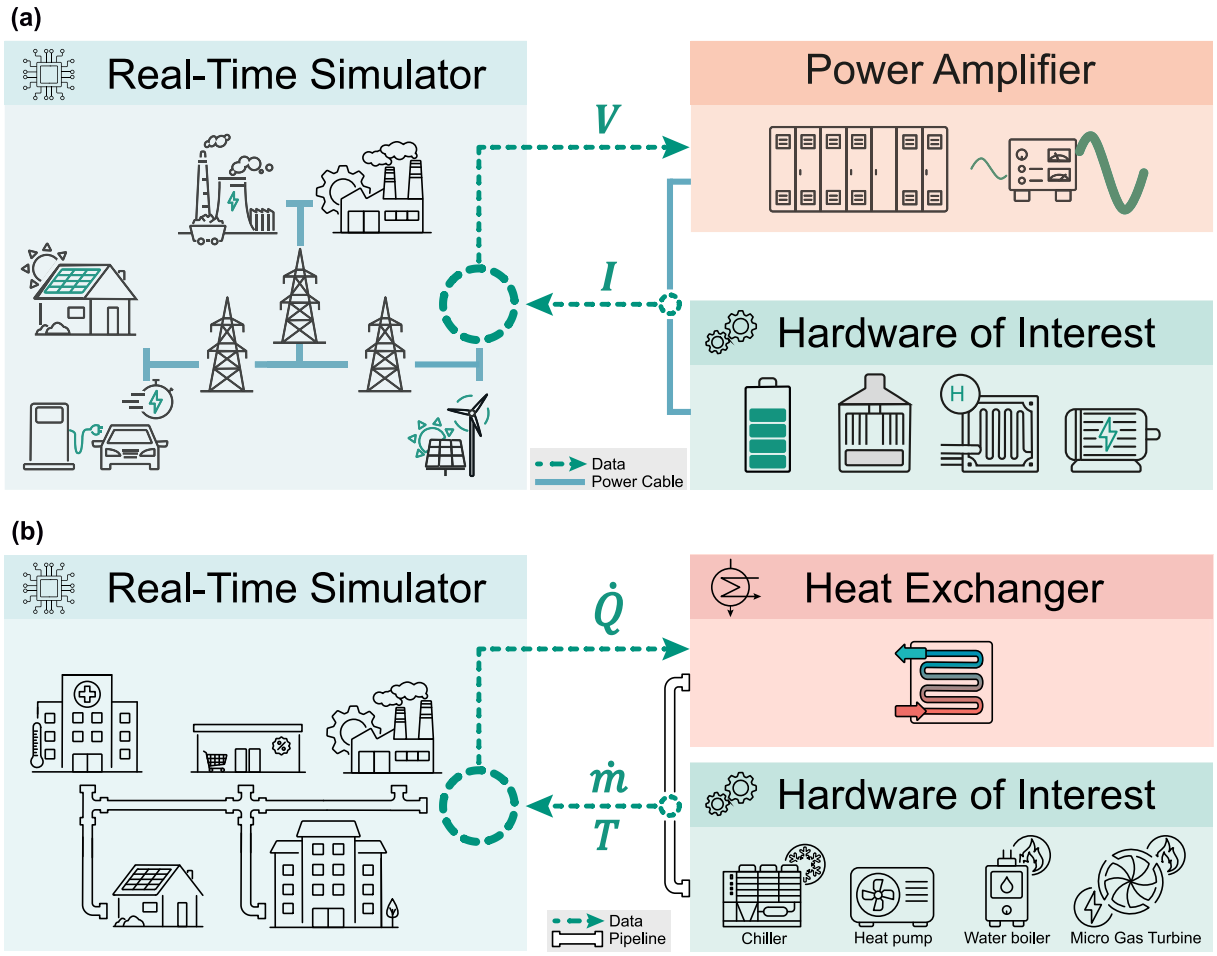

Fig. 1. (a) Generic scheme of PHIL, (b) Generic scheme of THIL [32].

the simulation and the PLCs on the hardware side. The DHW emulator operated in open loop based on the simulation's predefined load profile (water temperature and flow rate), whereas in the space heating loop, the model sent setpoints for hot water return temperature and flow rate to the hardware, and the hardware fed back the measured supply and return water temperature and flow rate to the model.

Table 1 provides a summary of state-of-the-art research on HIL testing of thermal systems that has been discussed in the introduction and this section. Although considerable progress has been made in the application of HIL to thermal systems, there is still no standardized reference framework. In particular, most existing studies focus mainly on equipment performance and specific configurations for a dedicated application, without clearly defined sections for hardware, software, and interfaces, or providing a structured interface algorithm. Furthermore, as mentioned in the introduction, real-time communication between the model and the hardware is complex, requiring multiple communication interfaces and software to transmit data, which poses challenges for more complex models. Moreover, as shown in Table 1, existing studies rarely focus on validating the HIL load-tracking accuracy under rapid dynamics.

To address this gap and inspired by the PHIL method, this research proposes the concept of Thermal Hardware-in-the-Loop (THIL) as a reliable framework for the experimental evaluation of thermal systems. THIL enables interaction between a simulated thermal grid (e.g., a building's heating load) and physical thermal hardware (e.g., a boiler) via a real-time simulator and a thermal interface, such as a heat exchanger. The real-time simulator executes the model and enables bidirectional communication with the hardware, facilitating reliable data exchange between the MoI and the HoI. The model and the hardware are fully coupled, with a single time step used to run both in a closed-loop configuration. The present work can serve as a starting point toward the standardization of a reference setup for testing thermal equipment under realistic, reproducible conditions.

3. Thermal Hardware-in-the-Loop concept

Thermal Hardware-in-the-Loop (THIL) is an experimental methodology that enables realistic testing of thermal systems by combining simulated models with physical hardware in a closed-loop configuration. A THIL consists of Model of Interest (MoI), Hardware of Interest (HoI), and Thermal Interface. Fig. 1 illustrates generic schemes of PHIL and THIL, which are comparable. In the proposed THIL configuration, the MoI is a thermal grid, i.e., a space heating/cooling load of a building, which is executed on a real-time simulator, and the HoI is a thermal source, instead of an electrical load and source, and the interface is a heat exchanger instead of a power amplifier. The heat exchanger and the thermal source are connected through pipes. Communication between the simulated and physical domains is managed via analog signals using the real-time simulator, which sends control signals to the hardware and receives feedback signals to close the loop and update the simulation. Fig. 1(a) shows the Voltage-Type Ideal Transformer Method (V-ITM) interface algorithm for PHIL in which the real-time simulator sends the voltage signal to the amplifier, the amplifier applies the real voltage on the HoI, and the measured current is fed back to the model in the simulator. The V-ITM method is presented as an example to illustrate that the voltage and current are transferred between the model and hardware in PHIL to establish a closed-loop communication. The power amplifier can also act as a current source in the Current-Type

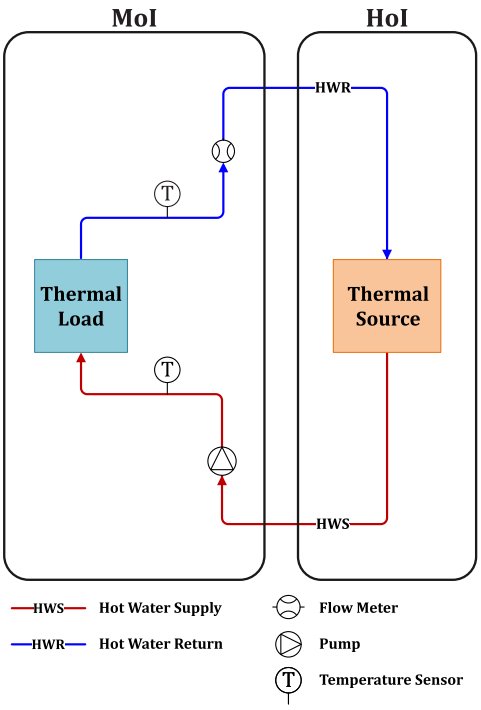

Fig. 2. Ideal coupling of source and load.

Ideal Transformer Method (C-ITM) interface algorithm, in which the current is forward path, and the voltage is feedback. In THIL, as shown in Fig. 1(b), the thermal load is calculated in the real-time simulator and sent to the heat exchanger, the heat exchanger applies the real load on the thermal source, and the measured mass flow rate and temperature of the fluid at the outlet of the thermal source are fed back to the model. Depending on the type of heat exchanger, the thermal load in the forward path should be transferred to another parameter that can be directly adjusted to change the load, e.g., fan speed, pump speed, etc., which will be discussed in Section 4.

The proposed THIL framework can be applied in diverse applications within the energy sector. The performance of heating and cooling sources, such as water boilers, heat pumps, micro-gas turbines, fuel cells, chillers, district heating substations, etc., as well as their control strategies, can be evaluated using the THIL approach. The real-time simulator has the advantage of running complex thermal models in real time, e.g., a distributed heating and cooling load network of a building or a district thermal network model that includes a building thermal model, and substations with all components modeled in detail. In addition, THIL can be integrated into a multi-physics HIL arrangement as addressed in [32]; for example, a micro-CHP unit or an HVAC unit can be tested simultaneously with PHIL on the electrical side and THIL on the thermal side. This coupled testing enables assessment of both electrical and thermal performance to identify operating points that maximize system efficiency. The following section provides further details on THIL's working principles and the proposed interface algorithm to enable closed-loop interaction between the load and the source.

4. Thermal Hardware-in-the-Loop interface algorithm

This section addresses the interface algorithm for the THIL arrangement introduced in the previous section. As this paper investigates the heating mode of the THIL, a space heating load of a residential building with a radiator is considered as the MoI, and a water heater is the HoI. Fig. 2 shows the ideal coupling of source and load, in which they are connected directly, whereas in THIL the interface enables the load and source interaction, as illustrated in Fig. 3.

Fig. 3 shows a schematic of the THIL interface algorithm. As can be seen, the interface consists of a PI controller and a thermal interface, which is a water-to-air cooling heat exchanger. The PI controller and the MoI are executed on a real-time simulator, while the thermal interface and the HoI are physical components connected by pipes.

In the MoI, the hot water with mass flow rate of $\dot{m}_{MoI}$ and temperature of $T_{s,MoI}$ passes through the simulated load, and its temperature decreases to $T_{r,MoI}$. With the specified temperature difference, the load

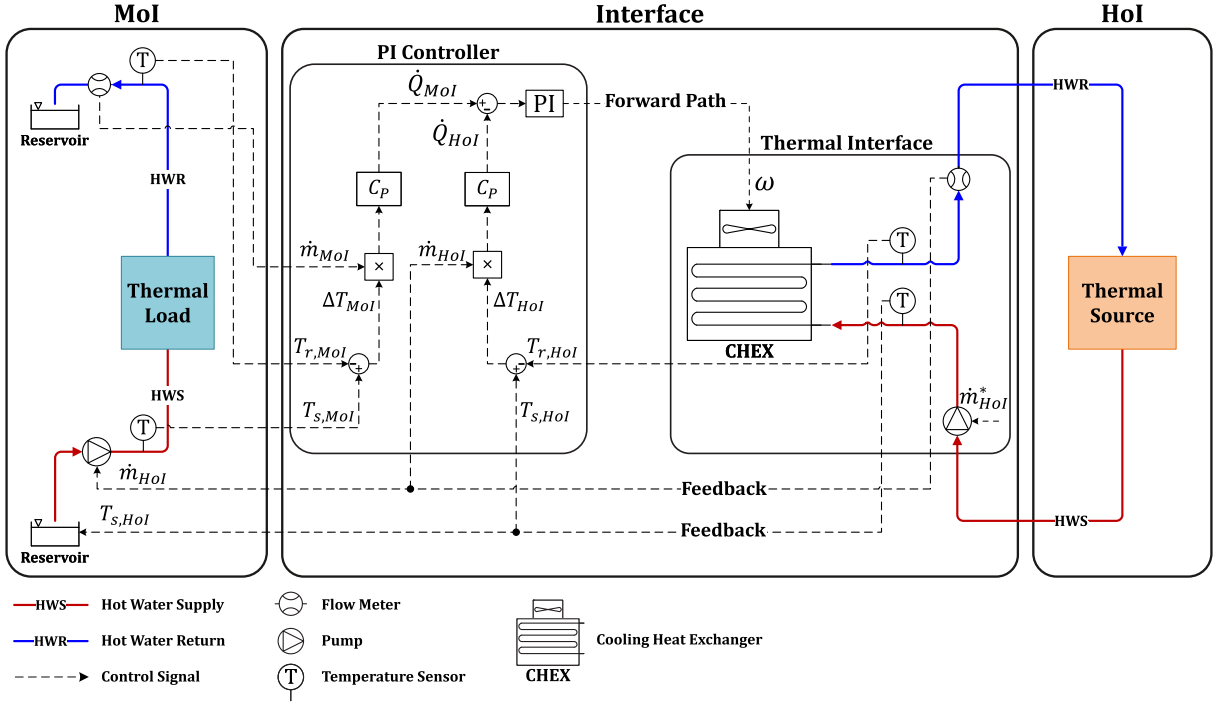

Fig. 3. THIL interface algorithm.

in the MoI ($\dot{Q}_{MoI}(W)$) is calculated as follows:

$$\dot{Q}_{MoI} = \dot{m}_{MoI} C_P \Delta T_{MoI} = \dot{m}_{MoI} C_P (T_{s,MoI} - T_{r,MoI}) \quad (1)$$

where $\dot{m}_{MoI}$ is the hot water mass flow rate in the MoI (kg/s), C_P is the specific heat of water (J/(kgK)), $T_{s,MoI}$ is hot water supply temperature in the MoI (K), and $T_{r,MoI}$ is hot water return temperature in the MoI (K). A similar process occurs in the HoI, where the hot water flow passes through the cooling heat exchanger and its temperature decreases from $T_{s,HoI}$ to $T_{r,HoI}$. The thermal load in cooling heat exchanger ($\dot{Q}_{HoI}(W)$) is derived as follows:

$$\dot{Q}_{HoI} = \dot{m}_{HoI} C_P \Delta T_{HoI} = \dot{m}_{HoI} C_P (T_{s,HoI} - T_{r,HoI}) \quad (2)$$

where $\dot{m}_{HoI}$ is the hot water mass flow rate in the HoI (kg/s), $T_{s,HoI}$ is hot water supply temperature in the HoI (K), and $T_{r,HoI}$ is hot water return temperature in the HoI (K).

The setpoint water mass flow rate $\dot{m}^*_{HoI}$ is manually adjusted in the real-time simulation user interface during the test, and the command is sent to the pump. It represents a situation in which the building resident increases or decreases the water flow through the radiator to achieve the desired room temperature. The measured mass flow rate $\dot{m}_{HoI}$ is then sent back to the MoI along with the measured hot water supply temperature $T_{s,HoI}$ as feedback. Consequently, as illustrated in Fig. 3, the same flow ($\dot{m}_{HoI}$, $T_{s,HoI}$) enters both the cooling heat exchanger at the interface and the load in the MoI. The cooling heat exchanger must act in a way that $T_{r,HoI}$ remains the same as $T_{r,MoI}$, so that the cooling heat exchanger imposes the desired thermal load on the HoI. As mentioned in Section 3, the thermal load in the MoI should be transferred to another parameter and sent to the heat exchanger to control the load that should be imposed on the HoI. To achieve this goal, as shown in Fig. 3, $\dot{Q}_{HoI}$ is compared to $\dot{Q}_{MoI}$ at each time step by the PI controller to adjust the cooling fan speed ω as forward path parameter in a way that the difference between these two loads tends towards zero. This closed-loop control of fan speed ensures accurate emulation of the MoI load in the experimental setup, with minimal error. As thermal systems have inherently slower dynamics than electrical systems, any potential controller instability does not pose a high risk of equipment failure before the system operator can take corrective action. Therefore, stability analysis and systematic tuning of the PI controller are not addressed in this paper.

As explained, this study examines THIL for heating hardware. It should be noted that the same approach can be applied to a cooling hardware using the same logic. Additionally, a water-to-water heat exchanger can be considered as a thermal interface instead of a water-to-air heat exchanger.

5. Software modeling

This section presents the THIL modeling in two subsections. First, the main components of THIL are described; then, the simulation results are presented and discussed.

5.1. Thermal Hardware-in-the-Loop modeling

The simulation is implemented in MATLAB/Simulink using the Simscape library with a discrete fixed-step solver. The simulation time is considered 3600 s with a time step of 0.1 s. The working fluid is water, with a constant supply temperature of 323.15 K, while its thermophysical properties are calculated at its mean temperature. Furthermore, it is assumed that all pipelines are ideally insulated, and the conductive thermal resistance of the pipe wall is negligible.

Table 2
Load model assumptions.

Parameter	Value
Total building living area	240 m^2
Total air volume	720 m^3
Total windows area	32 m^2
Surfaces exposed to ambient temperature (walls and roof)	496 m^2
Surfaces exposed to interior space (walls and floor)	480 m^2
Design ambient temperature	268.15 K
Design room temperature	293.15 K

Table 3
Cooling heat exchanger design parameters.

Parameter	Value
Cooling capacity	15.6 kW
Air flow rate	6259 m^3/h
Fan speed	1260 rpm
Air inlet/outlet temperature	35/42.6 °C
Water flow rate	1.36 m^3/h
Water inlet/outlet temperature	50/40 °C
Tube volume	$6.9e^{-3}$ m^3
Total fin surface area	74.6 m^2

5.1.1. Thermal load

A space heating model of a building with a radiator, supplied with hot water from the heat source while the building is exposed to ambient temperature, is simulated as a thermal load. The thermal grid of the load model is developed using a MATLAB library that simulates one-dimensional heat transfer (perpendicular to the heat transfer surface) between indoor air and a constant ambient temperature through walls, roofs, and windows, while accounting for their thermal mass. The radiator is modeled as a pipe in contact with the room air, and heat transfer due to infiltration is also considered. The minimum ambient temperature of 268.15 K is considered to calculate the maximum steady-state load, while the desired room temperature is 293.15 K. Table 2 summarizes the assumptions of the load model.

Taking these assumptions into account, the thermal load of the building is 10800 W. Assuming the maximum temperature drop of water at maximum load is 10 K, the hot water mass flow rate can be calculated as follows:

$$\dot{m}_{MoI} = \dot{Q}_{MoI} / C_P \Delta T_{MoI} \quad (3)$$

5.1.2. Thermal source

A hot water boiler from the MATLAB library is considered as a thermal source. The boiler structure is assumed to be similar to an instant water boiler. A furnace is connected to the gas side of a heat exchanger, and the heat generated from the burning of gas is transferred to the water flowing in the tube. The boiler supplies hot water at a constant temperature of 323.15 K, considering a switch on the furnace which is controlled by the hot water supply temperature to regulate the fuel mass flow rate.

5.1.3. Thermal interface

Since in the present study, THIL is developed for heating mode, the interface should be a cooling heat exchanger that acts the same as the simulated load. Therefore, as mentioned in Section 4, a water-to-air cooling heat exchanger is simulated as an interface. The heat exchanger arrangement is cross-flow, in which the air flow passes through parallel hot water tubes. The parameters of the heat exchanger in the model are based on the heat exchanger available in the lab. Table 3 addresses some of the important parameters of the heat exchanger.

5.2. Simulation results

In this section, simulation results of the study are presented and analyzed in terms of hot water return temperature, thermal load, fan speed, and room temperature. In the results, the term Ideal refers to the ideal configuration in which the thermal source and thermal load are directly connected and interact without an interface, as shown in Fig. 2. In contrast, in THIL, the MoI serves as a reference that the HoI follows via the thermal interface. Two case studies have been considered to evaluate THIL capabilities:

- Case Study I: The water mass flow rate is constant throughout the simulation time.
- Case Study II: The water mass flow rate changes a few seconds after a step change in ambient temperature to reduce the changes in room temperature.

5.2.1. Case Study I

As illustrated in Fig. 4(a) in the first case study, the plots have been divided into three zones over time. In the primary transient zone, the simulation starts from an initial condition, and it approaches a steady state. The ambient temperature is set to 278.15 K and the water mass flow rate is adjusted to 0.258 kg/s. As the simulation begins, hot water flow passes through the load in the MoI and cooling heat exchanger in the interface; therefore, its return temperature gradually decreases from 323.15 K to less than 314 K (Fig. 4(b)), and as a consequence the thermal load increases as shown in Fig. 5(b). The influence of the PI controller on the return temperature and thermal load is more evident at the beginning of the simulation in Figs. 4(b) and 5(b), where the water return temperature, and consequently the thermal load, oscillates around the reference profile of the MoI. This effect is due to the changes in fan speed as the output of the PI controller, which is adjusted to minimize the difference between the thermal load in the MoI and the HoI, as shown in Fig. 6. At $t = 1200$ s, the ambient temperature decreases from 278.15 K to 268.15 K as a step change to increase the load, and it returns to 278.15 K at $t = 2400$ s to decrease the load. The step change in ambient temperature is imposed on the MoI to evaluate the response of THIL to load changes. As shown in Fig. 7, during this period, the thermal load varies according to the hot water return temperature, which is controlled by the fan speed. It can be seen in Figs. 4(c),(d) and 5(c),(d) that the difference of return temperature and thermal load between the HoI and the MoI is negligible with a small shift at the load change points. This shift depends on how fast the PI controller responds to changes in the MoI load and how rapidly the heat exchanger adjusts the water return temperature, and consequently, the HoI thermal load. Rapid oscillations of the thermal load in Fig. 5(c),(d) result from the switching action of the heat source to keep the supply temperature constant. The maximum relative error between the HoI and the ideal thermal load from $t = 1200$ s to 3600 s is 0.04%, indicating that the simulated THIL can accurately replicate the Ideal configuration. Since the hot water mass flow rate is constant, it is evident in Fig. 7 that the room temperature changes significantly with changing ambient temperature as expected.

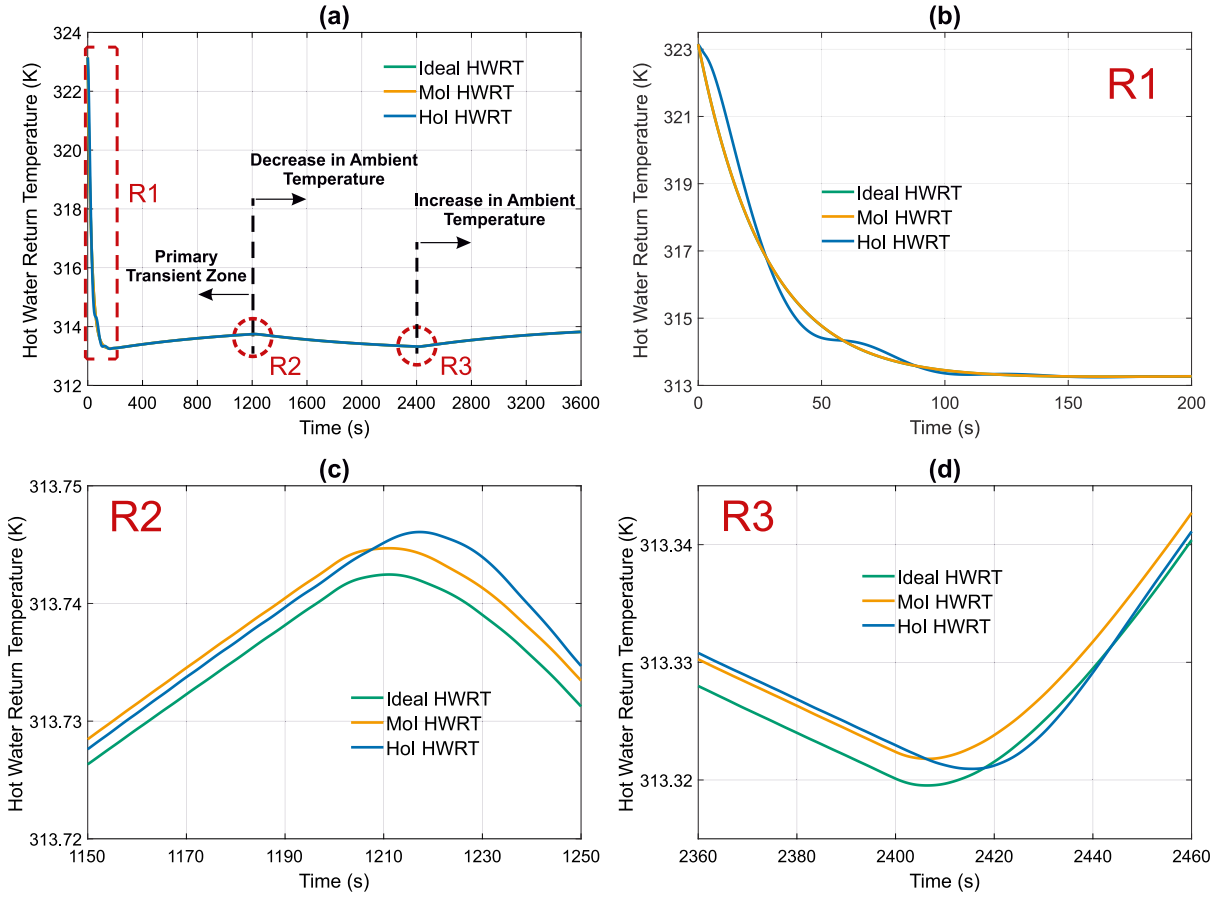

Fig. 4. Case Study I; (a) hot water return temperature variation versus time, (b) magnified view of region R1, (c) magnified view of region R2, (d) magnified view of region R3.

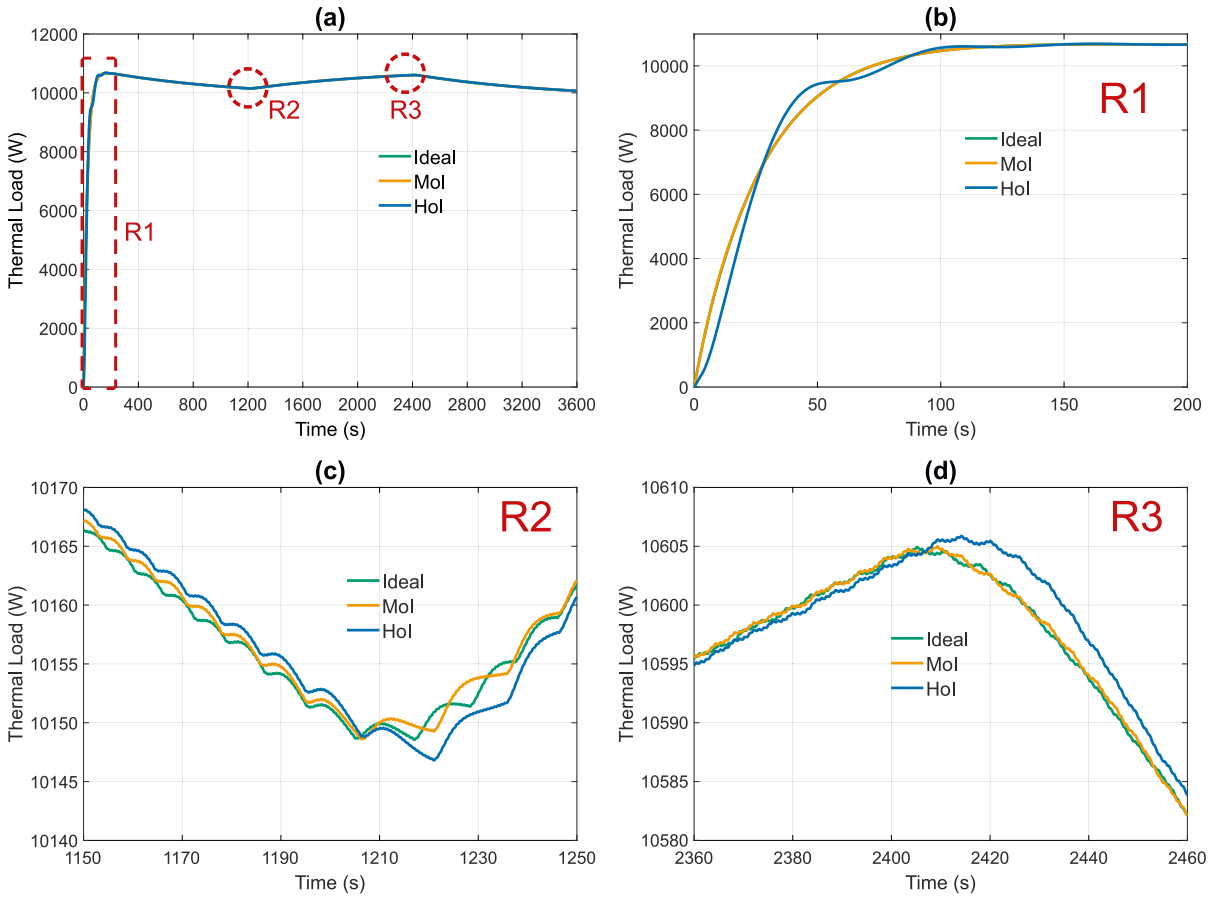

Fig. 5. Case Study I; (a) thermal load variation versus time, (b) magnified view of region R1, (c) magnified view of region R2, (d) magnified view of region R3.

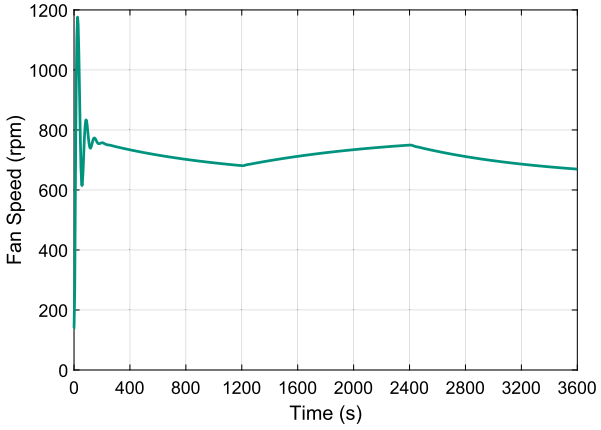

Fig. 6. Case Study I; fan speed variation versus time.

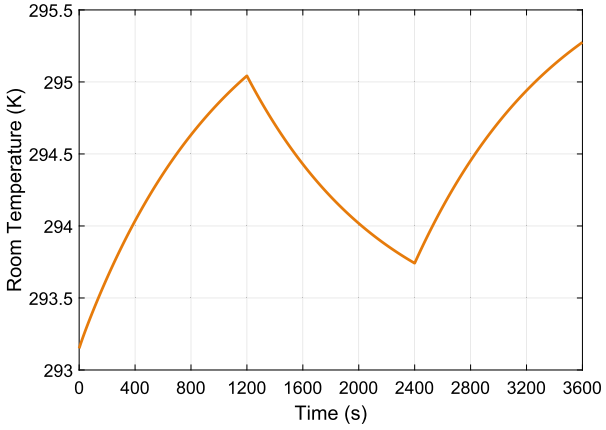

Fig. 7. Case Study I; room temperature variation versus time.

5.2.2. Case Study II

This section presents the simulation results of the second case study. In this case, the plots are divided into five zones over time, as illustrated in Fig. 8. In the primary transient zone, the ambient temperature is set to 278.15 K, the hot water mass flow rate is 0.167 kg/s, and the simulation is approaching its steady state. At t = 1000 s, the ambient temperature decreases to 268.15 K in the MoI. It can be seen in Fig. 9(b) that the thermal load increases gradually as the hot water return temperature decreases (Fig. 8(b)), while the water mass flow rate is constant. The HoI follows the decrement in water return temperature and an increase in thermal load since the PI controller increases the fan speed, as shown in Fig. 10. The room temperature also drops between t = 1000 and 1200 s, as illustrated in Fig. 11. As described in Section 4, considering a situation where the resident of the building increases the water flow rate in the radiator to reach the desired room temperature, at t = 1200 s, the water flow rate increases in 30 s to 0.258 kg/s with a command to the thermal interface and the measured flow rate is sent to the MoI compensating the room temperature drop. The thermal load in both the MoI and the HoI rises sharply to its peak due to the rapid increase in water flow rate, while the hot water return temperature requires more time to respond. As shown in Fig. 9(c), once the water flow rate reaches its maximum value at t = 1230 s, the thermal load approaches a steady state as the return temperature increases. A corresponding and desirable rise in room temperature is observed in Fig. 11. At t = 2000 s, the ambient temperature returns to its initial value of 278.15 K in the MoI, while the water mass flow rate is still 0.258 kg/s, and it is evident in Fig. 8(c) that the hot water return temperature gradually rises. This causes a decrease in thermal

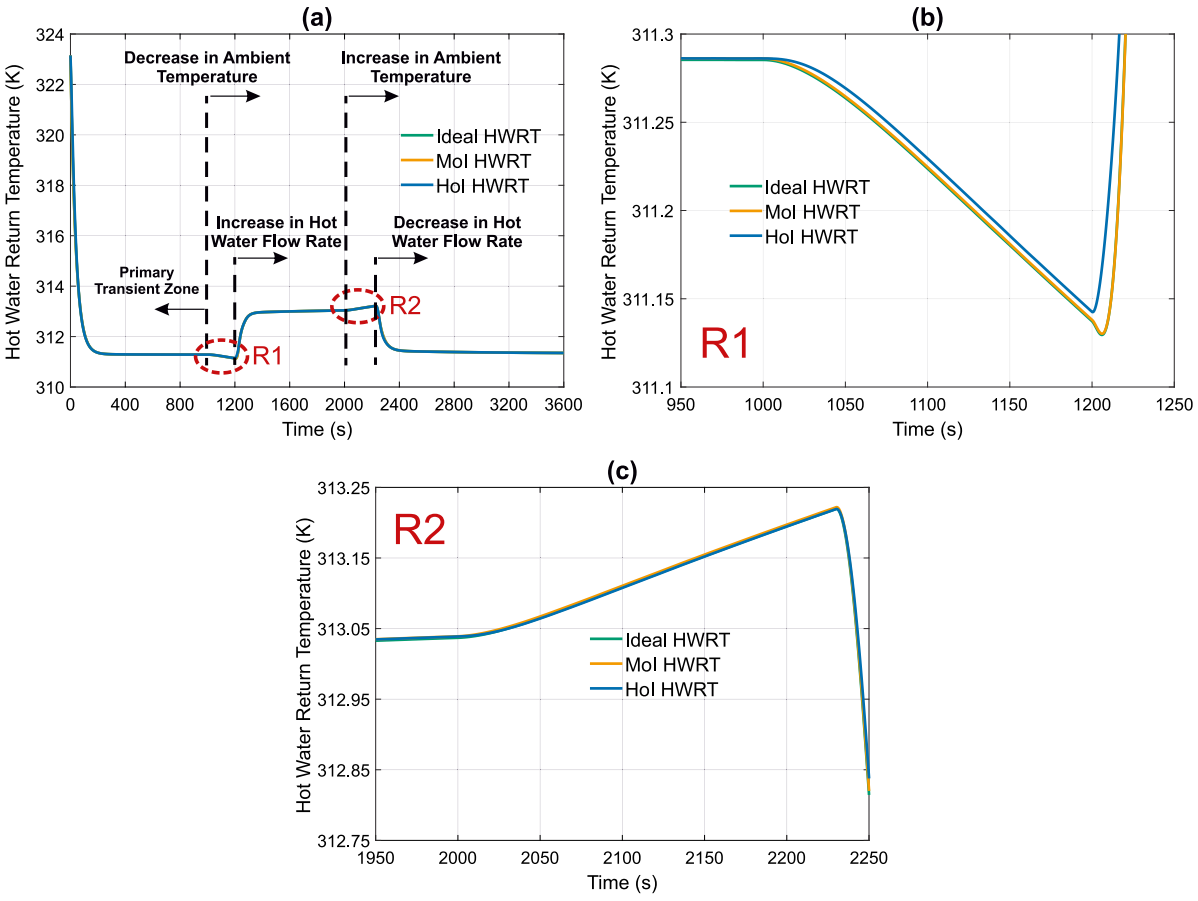

Fig. 8. Case Study II; (a) hot water return temperature variation versus time, (b) magnified view of region R1, (c) magnified view of region R2.

load (Fig. 9(d)) and a notable increase in room temperature (Fig. 11). With the same scenario of increasing the water flow rate, at $t = 2230$ s, the water mass flow rate returns to its initial value of 0.167 kg/s in 30 s. As a result, the thermal load decreases, and after reaching a minimum (Fig. 9(e)), it tends toward a steady state as the hot water return temperature drops. A downward trend in the room temperature in Fig. 11 is observed, with the temperature remaining around 293.15 K. Throughout the simulation, the fan speed tracks load changes to minimize the difference between the HoI and MoI loads, as illustrated in Fig. 10. The maximum relative error between the HoI and the ideal load from $t = 1000$ s to 3600 s is 0.8%, which shows that THIL is capable of creating the same behavior of ideal interaction between load and source with minimal error.

6. Experimental validation

The proposed THIL configuration is experimentally validated in this section. The main components of the THIL setup are introduced, and the experimental results are discussed.

6.1. Thermal Hardware-in-the-Loop setup

As shown in Fig. 12, there are three main components configuring this setup, including: a Real-time Simulator, a Thermal Source, and a Thermal Interface.

The real-time simulator (OPAL-RT OP4510) is employed to interface the simulated load with the physical hardware. Since the model is developed in MATLAB/Simulink, the OPAL-RT simulator is selected, as it provides a user-friendly interface to MATLAB via RT-LAB. The Simulink model is compiled within RT-LAB and executed on the real-time simulator, with a simulation time step of 0.01 s. Even though it is possible to conduct the experiments with a larger time step, the small time step enables capturing rapid dynamics, e.g., changes in fluid mass flow rate that can occur in a few seconds. Moreover, as mentioned in Section 3, THIL can contribute in a multi-physics test environment, e.g., parallel testing of the electrical and thermal side of a system under test. In such cases, the time step should be small enough to capture the electrical dynamics that are faster than the thermal dynamics. The simulator is equipped with analog and digital input/output (I/O) cards, which enable bidirectional signal exchange between the model and the hardware. In this study, only analog I/O cards are used, as all signals are analog voltage. Each analog I/O card can transmit or receive up to 16 signals simultaneously, facilitating efficient data transfer between the simulation and the experimental setup.

An instantaneous electric water heater with the rated power of 50 kW is used as the thermal source, which is supplied with three APS 15000 4-quadrant amplifiers, Spitzenberger & Spies. The power of the heater is adjusted by regulating the voltage via the amplifier's user interface. Additionally, as noted in software modeling, a water-to-air heat exchanger (GUNTNER GFHC WD 050.1/11-43) is employed as the thermal interface between the thermal load and the source. The general specifications of the heat exchanger are provided in Section 5.1.3. The fan speed of the heat exchanger is controlled via a voltage signal from the PI controller output in the real-time simulation to the fan actuator. An inline multistage centrifugal pump (Grundfos CRE 3-4 AAAE-HQQE) circulates the water, which is adjusted by a voltage signal from the real-time simulation console to provide the desired flow rate. The supply and return temperatures of hot water are measured by two temperature transmitters (IFM TA3317) at the inlet and outlet of the heat exchanger, respectively. In addition, a flow meter (IFM SM6000) on the return line from the heat exchanger to the water heater measures the hot water flow rate. All sensors are connected to the analog input

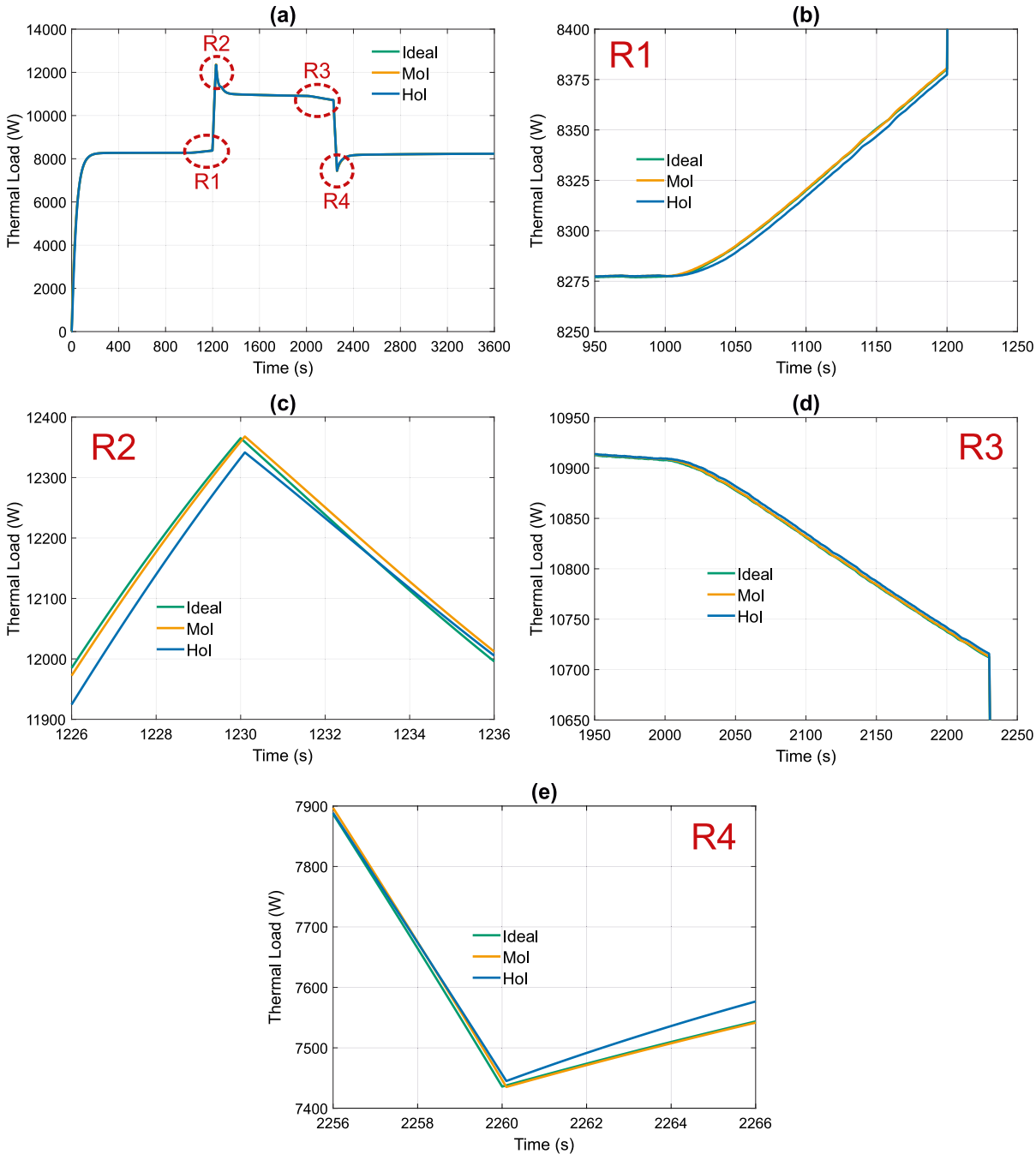

Fig. 9. Case Study II; (a) thermal load variation versus time, (b) magnified view of region R1, (c) magnified view of region R2, (d) magnified view of region R3, (e) magnified view of region R4.

card of the OPAL-RT simulator for data recording and monitoring. It should be noted that all sensors and the circulating pump are integrated with the cooling heat exchanger on a portable platform, forming the thermal interface, which enables easy connection to any thermal source compatible with this setup.

6.2. Experimental results

This section presents the experimental results of the two case studies introduced in Section 5.2. Unlike in simulations, where the system starts directly at the desired hot water supply temperature of 323.15 K, the experimental setup requires a warm-up period to reach this operating point. During this warm-up phase, the system runs in simulation mode. In this mode, the controller compares the simulated HoI load with the MoI setpoint, both executed in the real-time simulator, and the PI controller output is sent to the fan actuator to adjust the fan speed. Once the hot water supply temperature reaches approximately 323.15 K, the system switches to using the actual HoI load, generated by the cooling heat exchanger, and this real load is then sent to the PI controller for comparison with the setpoint. Data collection begins when the system reaches the operating temperature, and the actual HoI load is engaged. Therefore, all experimental plots in this section reflect system behavior after reaching the operating point and initiating real-time control.

This study is conducted on the assumption that the thermal source provides hot water at the desired supply temperature via an independent control system. Since the main focus of this study is to establish a closed-loop interaction between the thermal source and MoI via an

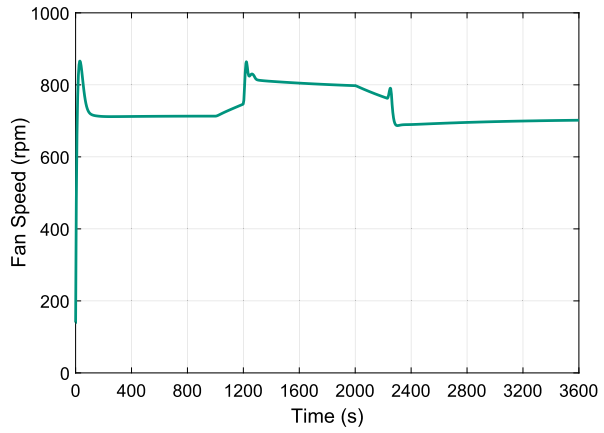

Fig. 10. Case Study II; fan speed variation versus time.

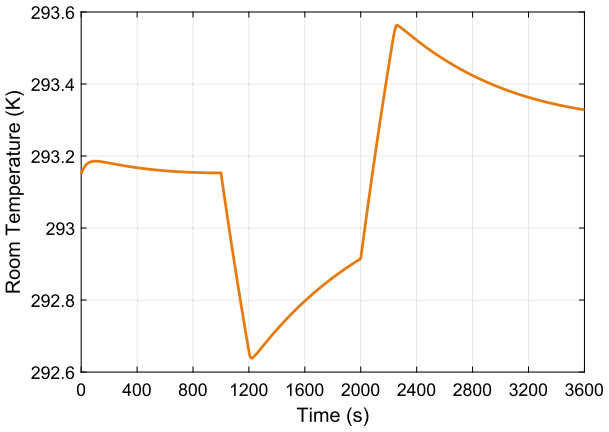

Fig. 11. Case Study II; room temperature variation versus time.

interface algorithm, a simpler approach, i.e., manual control of the thermal source, is employed. To keep the hot water supply temperature in a reasonable range around 323.15 K, the feeding voltage from the power amplifier to the electric heater is adjusted manually during the test via the power amplifier user interface.

6.2.1. Case Study I

Figs. 13–16 present the results of the first case study. The hot water supply temperature is between 322.68 K and 323.82 K, and is sent from the HoI to the MoI as one of the feedback signals. The water mass flow rate command is sent from the RT-LAB console to the pump, and the measured water mass flow rate, equal to 0.258 kg/s with some minor fluctuations in the order of 0.001 kg/s, is received in the MoI as the second feedback signal. At $t = 400$ s, ambient temperature changes from 278.15 K to 268.15 K and returns to 278.15 K at $t = 1600$ s in the MoI to change the reference load. As shown in Fig. 13, the hot water return temperature in the HoI perfectly matches the hot water return temperature in the MoI and in Fig. 14 the thermal load of the HoI follows the reference load of the MoI with the maximum relative error of 3% which means the fan speed of the cooling heat exchanger is adjusted properly by the PI controller. Since the hot water mass flow rate is constant, the room temperature changes significantly with changing the ambient temperature, demonstrating the same behavior as in the simulation (See Fig. 16). It should be noted that Fig. 15 illustrates the fan speed sent from the PI controller to the cooling heat exchanger as a forward path. The fan speed at the controller output is converted into a voltage signal and transmitted to the fan actuator, which adjusts the fan speed accordingly. Since this process involves a delay, the fan responds with a lag relative to the moment that the PI controller issues the control command. Therefore, to preserve PI controller stability, the controller parameters should be adjusted within the model so that the controller operates at a relatively low speed. Despite considering this limitation, the controller output exhibits fluctuations. This behavior is primarily due to variations in the input signal, as well as the continuous effort of the controller to minimize input deviations. In addition, the fan actuator can receive and apply control signals with a resolution of 0.1 V. This means that regardless of the precision of the signal generated by the PI controller, the actuator can only interpret and apply it in increments of 0.1 V.

6.2.2. Case Study II

Experimental results of the second case study are provided in this section. As in the first case study, the voltage applied to the electric heater is regulated to achieve the desired hot water supply temperature. However, since the mass flow rate also varies in this case, keeping the temperature close to the target value of 323.15 K is more challenging. As a result, the hot water supply temperature remains within a range of 321.44 K to 324.86 K, as shown in Fig. 17. At $t = 350$ s, the ambient temperature decreases from 278.15 K to 268.15 K; as a result, hot water return temperature decreases slightly, and as illustrated in Fig. 18, the thermal load rises gradually. It is evident in Fig. 20 that the room temperature drops significantly since the hot water mass flow rate is constant and equal to 0.17 kg/s. At $t = 560$ s, hot water mass flow rate increases to 0.263 kg/s in 30 s to compensate for the room temperature drop; consequently, the thermal load rises intensively at the beginning due to the slow dynamics of the water temperature. However, as illustrated in Fig. 17(b), the hot water return temperature increases over time, and the thermal load gradually converges to a steady state (Fig. 18(b)). It is notable that, as the flow rate increases, the room temperature rises; however, beyond a certain point, it declines again with a more gradual slope. This behavior can be attributed to a slight decrease in the hot water supply temperature resulting from the increased flow rate, which limits the system's ability to further raise the room temperature. However, the room temperature remains close to the desired 293.15 K. At $t = 1350$ s, the ambient temperature returns to 278.15 K, which results in a slight decrease in thermal load and a significant increase in room temperature. At $t = 1590$ s, the hot water mass flow rate is set to its initial value of 0.17 kg/s in 30 s to keep the room temperature close to the desired 293.15 K. It can be observed that the thermal load decreases significantly and, as the hot water return temperature drops (Fig. 17(c)), the thermal load converges to a steady state (Fig. 18(c)). Fig. 19 shows that during the whole experiment, the fan speed is also regulated effectively to minimize the deviation between the HoI and the reference load in the MoI, with the maximum relative error of 7.6%.

In conclusion, the experimental results demonstrate that the proposed THIL setup accurately emulates the heating load, even with step changes in ambient temperature in the load model that impose relatively high dynamics on the system. The obtained results validate the THIL concept developed in this study. The same strategy can be extended to assess cooling systems and the interaction between cooling sources and loads. Depending on the capacity of the system under test and the magnitude of the target load, a water-to-water heat exchanger can be used as the thermal interface instead of a water-to-air heat exchanger. In such cases, the pump speed on the secondary side of the heat exchanger would serve as the forward path instead of the fan speed.

6.2.3. Measurement uncertainty

The uncertainty propagation from independent variables $(x_1, x_2, \ldots, x_n)$ to a function $(F(x_1, x_2, \ldots, x_n))$ is calculated as follows [33]:

$$u_F = \sqrt{(\frac{\partial F}{\partial x_1} u_{x_1})^2 + (\frac{\partial F}{\partial x_2} u_{x_2})^2 + \cdots + (\frac{\partial F}{\partial x_n} u_{x_n})^2} \tag{4}$$

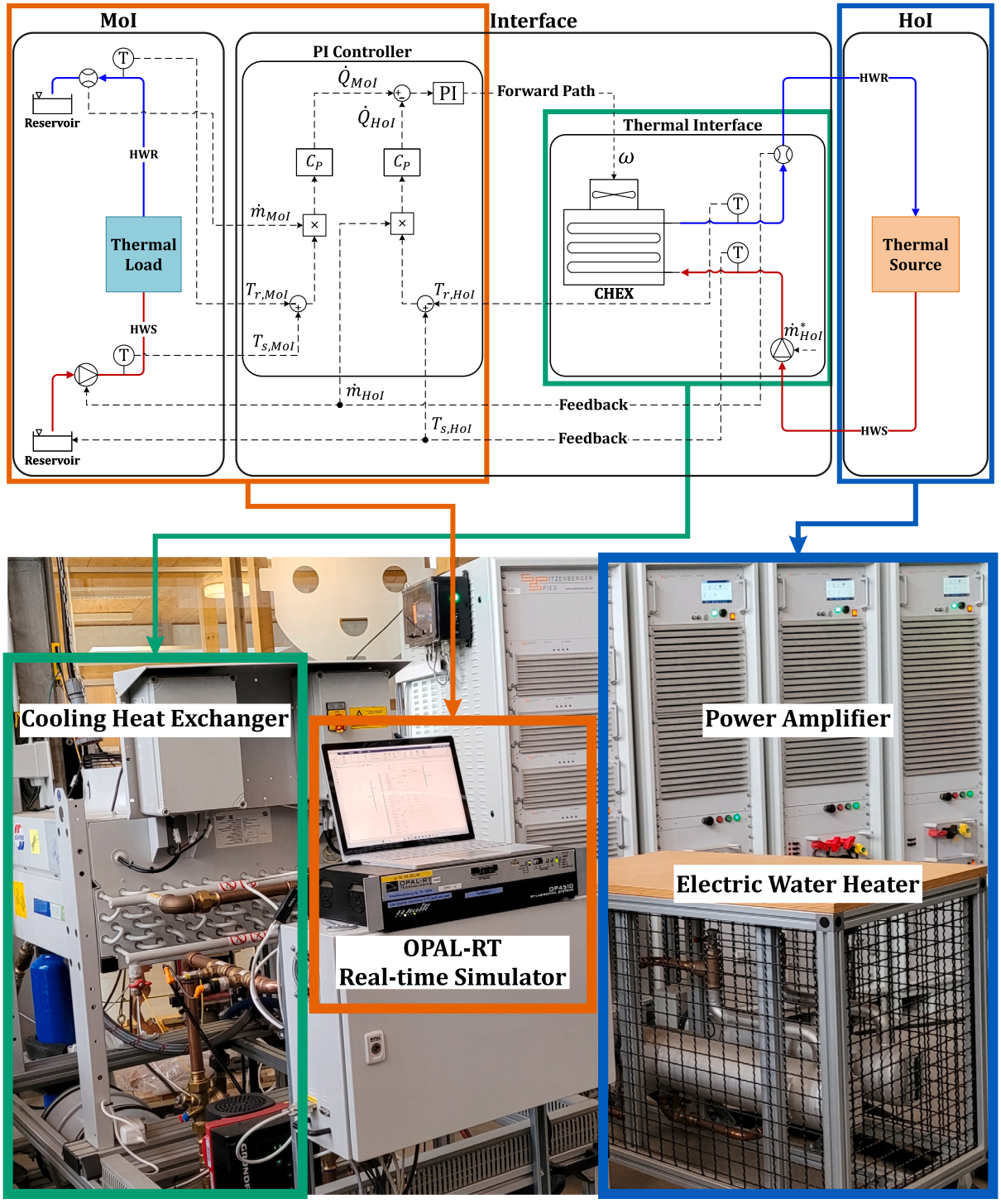

Fig. 12. THIL setup.

Accordingly, uncertainty in the thermal load in the experimental setup based on the flow rate and the temperature difference is given by Eq. (5):

$$u_{\dot{Q}_{HoI}} = \sqrt{\left(\frac{\partial \dot{Q}_{HoI}}{\partial \dot{m}_{HoI}} u_{\dot{m}_{HoI}}\right)^2 + \left(\frac{\partial \dot{Q}_{HoI}}{\partial \Delta T_{HoI}} u_{\Delta T_{HoI}}\right)^2} \tag{5}$$

Where $u_{\dot{m}_{HoI}}$ and $u_{\Delta T_{HoI}}$ are the uncertainties in the measured hot water flow rate and temperature difference, respectively. By applying partial derivatives in Eq. (5), the uncertainty in the thermal load is expressed as Eq. (6):

$$u_{\dot{Q}_{HoI}} = \dot{Q}_{HoI} \sqrt{\left(\frac{u_{\dot{m}_{HoI}}}{\dot{m}_{HoI}}\right)^2 + \left(\frac{u_{\Delta T_{HoI}}}{\Delta T_{HoI}}\right)^2} \tag{6}$$

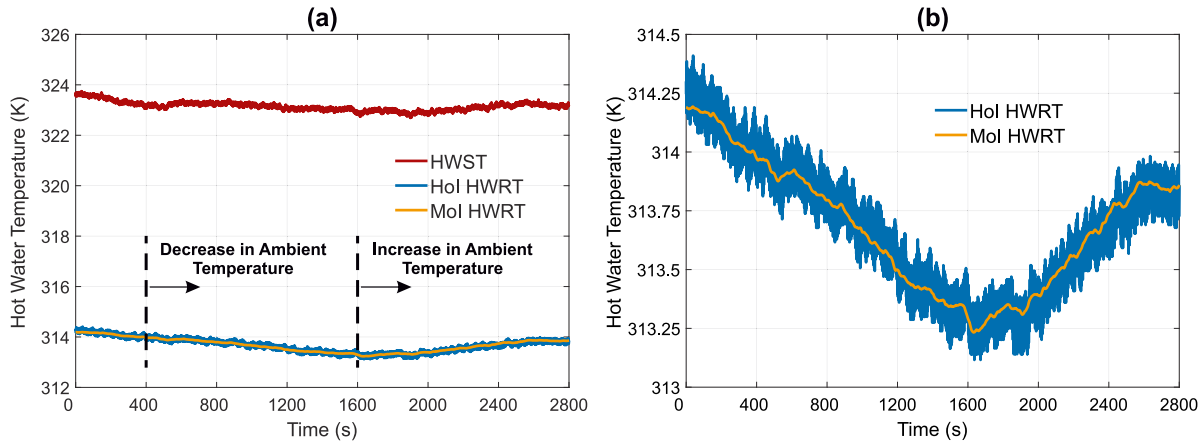

Fig. 13. Case Study I; (a) hot water temperature variation versus time, (b) hot water return temperature variation versus time.

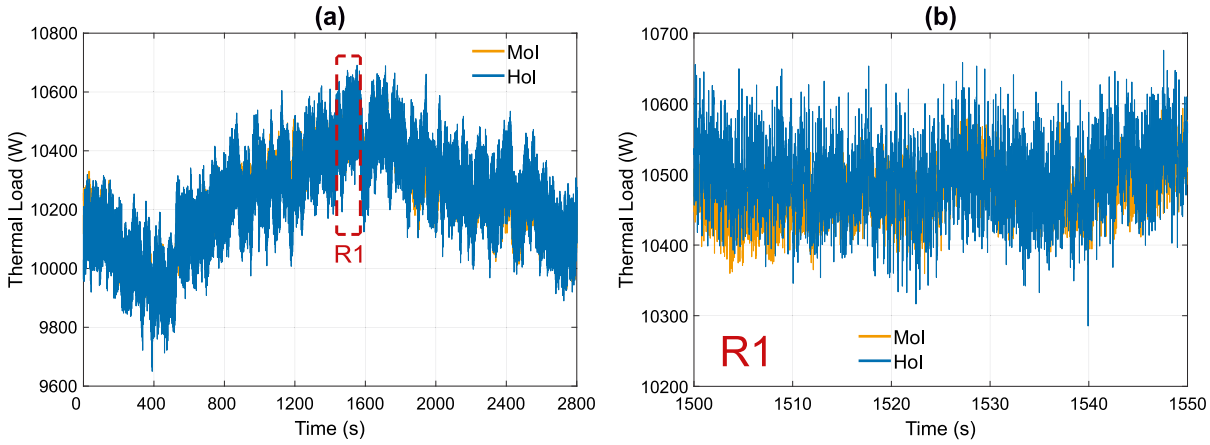

Fig. 14. Case Study I; (a) thermal load variation versus time, (b) magnified view of region R1.

Table 4
Measurement uncertainty.

Case Study	$\dot{m}_{HoI}$ (kg/s)	ΔT_{HoI} (K)		$\dot{Q}_{HoI}$ (W)	
		min	max	min	max
I	0.258 ± 0.0041	8.9 ± 0.57	9.8 ± 0.57	9623 ± 634	10663 ± 638
II	0.17 ± 0.0034 0.263 ± 0.0042	11.4 ± 0.57 9.1 ± 0.57	12.2 ± 0.57 9.9 ± 0.57	8110 ± 437 10051 ± 647	8709 ± 442 10883 ± 650

The uncertainties in temperature and flow rate are calculated based on the sensors' datasheets. As an example, in the first case study, for the mass flow rate of 0.258 kg/s, the uncertainty is calculated ±0.0041 kg/s. The uncertainty in the measured temperature is ±0.4 K, therefore, based on Eq. (4), the uncertainty in the temperature difference is approximately ±0.57 K. Considering the minimum and maximum temperature difference in the first case study, the minimum and maximum thermal loads are 9623 W and 10663 W, with uncertainties of ±634 W and ±638 W, respectively. Table 4 provides the measurement uncertainties for the two case studies at each constant mass flow rate for the minimum and maximum temperature difference.

7. Conclusion

The integration of energy systems and the significant role of thermal devices in the energy grid highlight the need for a flexible, accurate testing method to evaluate thermal equipment and their control strategies. This study presents a novel digital real-time simulator (DRTS)-based Thermal Hardware-in-the-Loop (THIL) concept as a reliable platform for testing thermal equipment, consisting of Model-of-Interest (MoI), Hardware-of-Interest (HoI), and thermal interface. It emphasizes a feasible interface algorithm that enables closed-loop interaction between thermal sources and loads. A PI controller-based load tracking is integrated into the interface algorithm to improve the accuracy of load emulation.

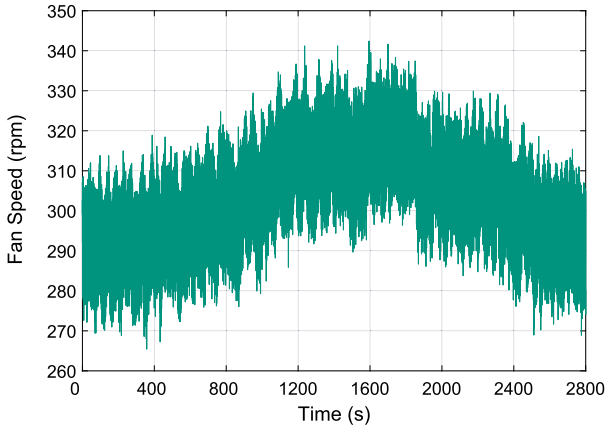

Fig. 15. Case Study I; fan speed variation versus time.

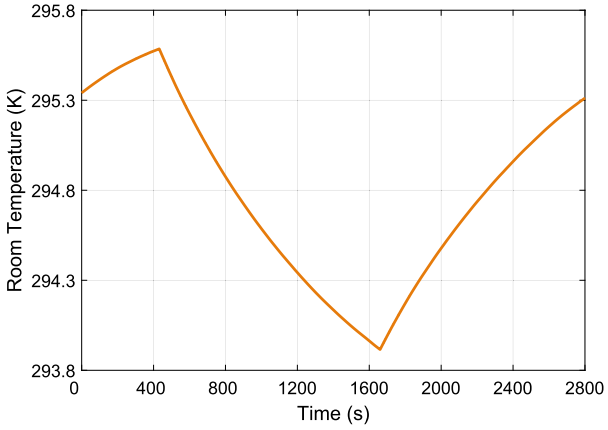

Fig. 16. Case Study I; room temperature variation versus time.

Two case studies using a residential space heating model are simulated in MATLAB/Simulink and experimentally validated. In the experiments, the load model is executed on a real-time simulator, which also manages bidirectional communication between the simulation and the hardware, as well as data acquisition. The simulation results show that the proposed THIL configuration accurately follows the reference load in the MoI, replicating the ideal interaction between the load and the source. The maximum relative errors between the thermal load emulated with THIL and the ideal thermal load are 0.04% and 0.8% for the two case studies, respectively. The experimental THIL setup also closely tracks the reference thermal load, with maximum relative errors of 3% and 7.6% for the two case studies, respectively. The measurement uncertainty is approximately 5 to 6.5%.

The difference between the simulation and experimental results can mainly be attributed to practical hardware limitations, including fan actuation delay, finite control signal resolution, and fan inertia, which are not present in the idealized simulation environment. Nevertheless, the experimental results demonstrate that the proposed THIL concept offers a reliable approach for coupling a simulated thermal load with real thermal hardware via a real-time simulator and a heat exchanger. Moreover, the digital real-time simulator provides a powerful environment for modeling complex networks, enables easier communication and data management than in previous studies, and facilitates testing integrated energy systems on a single platform in the future.

The proposed concept can serve as a guide for future THIL test benches and for further development toward standardized experimental frameworks for thermal systems. Future work may extend the proposed framework to more complex thermal networks and to advanced control strategies across a broader range of operating conditions, and integrate it into multi-physics HIL testing frameworks.

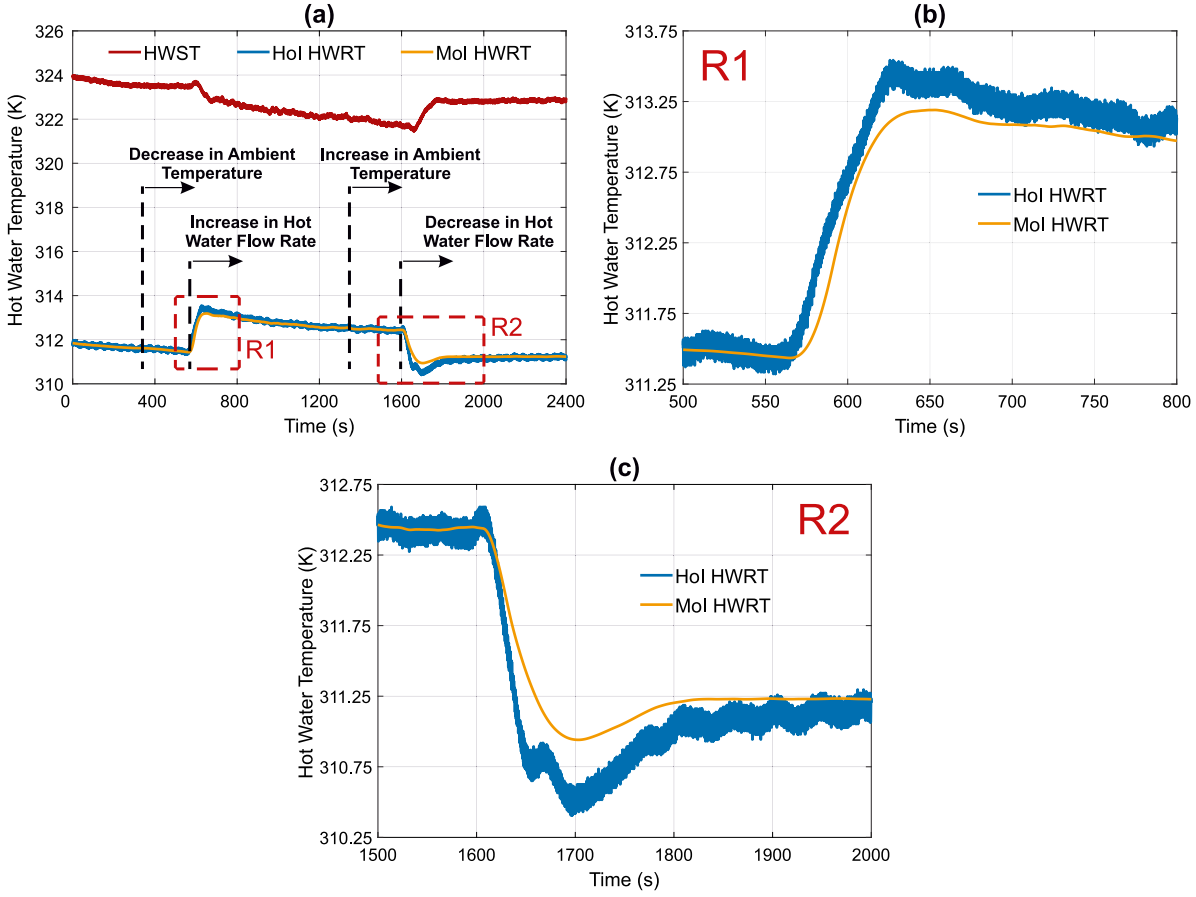

Fig. 17. Case Study II; (a) hot water temperature variation versus time, (b) magnified view of region R1, (c) magnified view of region R2.

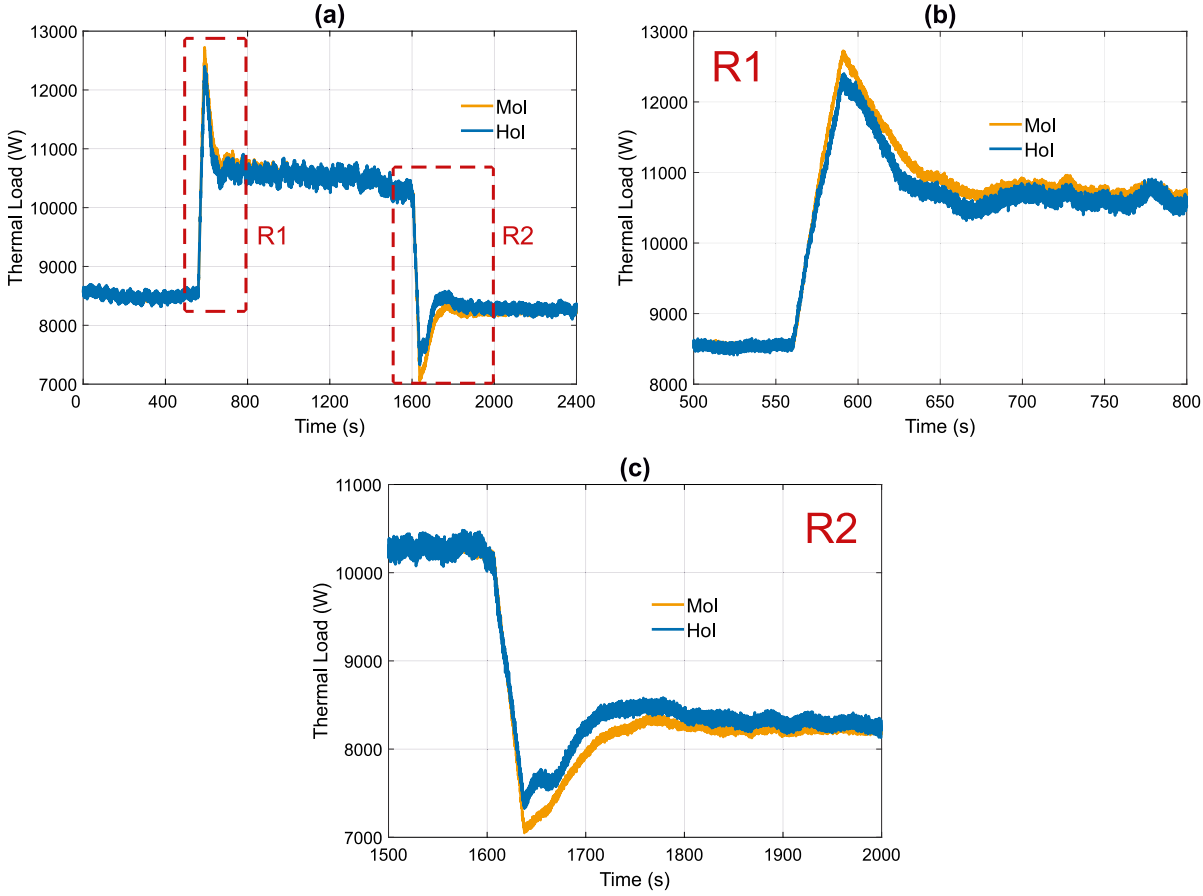

Fig. 18. Case Study II; (a) thermal load variation versus time, (b) magnified view of region R1, (c) magnified view of region R2.

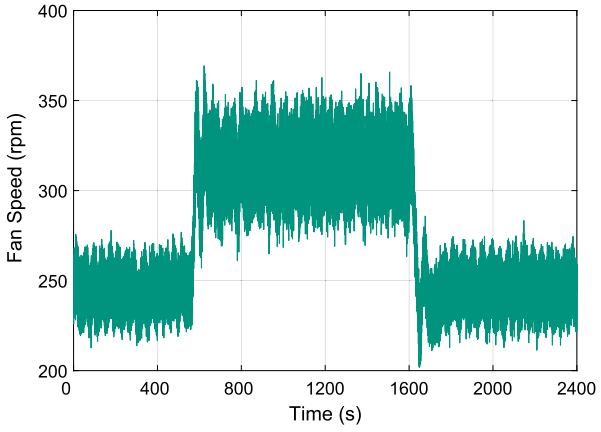

Fig. 19. Case Study II; fan speed variation versus time.

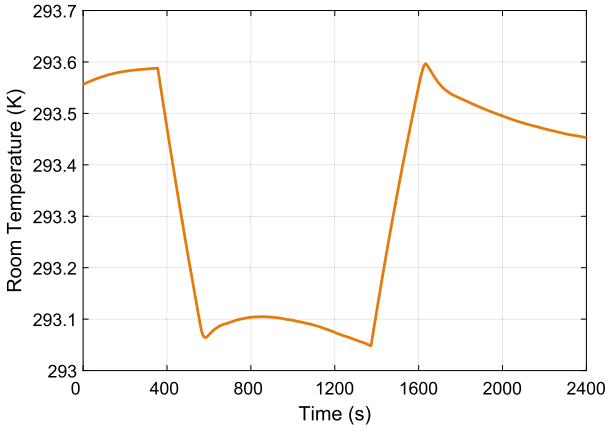

Fig. 20. Case Study II; room temperature variation versus time.

CRediT authorship contribution statement

Nima Ghorbani: Writing – review & editing, Writing – original draft, Visualization, Validation, Software, Methodology, Investigation, Formal analysis, Data curation, Conceptualization. **Fargah Ashrafidehkordi:** Writing – review & editing, Visualization, Validation, Supervision, Software, Project administration, Methodology, Investigation, Data curation. **Veit Hagenmeyer:** Writing – review & editing, Supervision, Resources. **Giovanni De Carne:** Writing – review & editing, Validation, Supervision, Resources, Project administration, Methodology, Investigation, Funding acquisition, Formal analysis, Conceptualization.

Declaration of generative AI and AI-assisted technologies in the manuscript preparation process

During the preparation of this work, the authors used ChatGPT (OpenAI) in order to improve the grammar and clarity of the manuscript. After using this tool/service, the authors reviewed and edited the content as needed and take full responsibility for the content of the published article.

Declaration of competing interest

The authors declare that they have no known competing financial interests or personal relationships that could have appeared to influence the work reported in this paper.

Acknowledgments

This work was supported in part by Helmholtz Association, Germany through the program "Energy System Design" and in part by Helmholtz Young Investigator Group "Hybrid Networks" under Grant VH-NG-1613. This funding source had no involvement in the study design, collection, analysis and interpretation of data, writing of the report, and decision to submit the article for publication.

Data availability

Data will be made available on request.

References

[1] Fagcang H, Stobart R, Steffen T. A review of component-in-the-loop: Cyber-physical experiments for rapid system development and integration. Adv Mech Eng 2022;14(8):16878132221109969.

[2] Soeiro LGG, Filho BJC. Vehicle power system modeling and integration in Hardware-in-the-Loop (HIL) simulations. Machines 2023;11(6):605.

[3] Walica D, Noskievič P. Application of the MiL and HiL simulation techniques in Stewart platform control development. Appl Sci 2022;12(5):2323.

[4] Mihalič F, Truntič M, Hren A. Hardware-in-the-loop simulations: A historical overview of engineering challenges. Electronics 2022;11(15):2462.

[5] P2004/D3, Oct 2024 - IEEE draft standard Hardware-in-the-Loop (HIL) simulation based testing of electric power apparatus and controls. IEEE; 2024.

[6] Lauss GF, Faruque MO, Schoder K, Dufour C, Viehweider A, Langston J. Characteristics and design of power hardware-in-the-loop simulations for electrical power systems. IEEE Trans Ind Electron 2015;63(1):406–17.

[7] Edrington CS, Steurer M, Langston J, El-Mezyani T, Schoder K. Role of power hardware in the loop in modeling and simulation for experimentation in power and energy systems. Proc IEEE 2015;103(12):2401–9.

[8] Ashrafidehkordi F, Kottonau D, De Carne G. Multi-rate discrete domain modeling of power hardware-in-the-loop setups. IEEE Open J Power Electron 2023;4:539–48.

[9] Steurer M, Edrington CS, Sloderbeck M, Ren W, Langston J. A megawatt-scale power hardware-in-the-loop simulation setup for motor drives. IEEE Trans Ind Electron 2009;57(4):1254–60.

[10] Dibos S, Pesch T, Benigni A. Individual versus grid-connected thermal systems: Impact on grid infrastructures and energy supply. In: 2024 open source modelling and simulation of energy systems. OSMSES, IEEE; 2024, p. 1–6.

[11] Langner F, Kovačević J, Zwickel P, Dengiz T, Frahm M, Waczowicz S, Çakmak HK, Matthes J, Hagenmeyer V. Coordinated price-based control of modulating heat pumps for practical demand response and peak shaving in building clusters. Energy Build 2024;324:114940.

[12] Kohlhepp P, Harb H, Wolisz H, Waczowicz S, Müller D, Hagenmeyer V. Large-scale grid integration of residential thermal energy storages as demand-side flexibility resource: A review of international field studies. Renew Sustain Energy Rev 2019;101:527–47.

[13] Frahm M, Dengiz T, Zwickel P, Maaß H, Matthes J, Hagenmeyer V. Occupant-oriented demand response with multi-zone thermal building control. Appl Energy 2023;347:121454.

[14] Langner F, Matthes J, Hagenmeyer V. Distributed model predictive control for district heating networks considering building and network flexibility. Energy 2026;140746.

[15] Delgado ML, Jiménez-Hornero JE, Vázquez F. Design, implementation and validation of a hardware-in-the-loop test bench for heating systems in conventional coaches. Appl Sci 2023;13(4):2212.

[16] De La Cruz AT, Riviere P, Marchio D, Cauret O, Milu A. Hardware in the loop test bench using modelica: A platform to test and improve the control of heating systems. Appl Energy 2017;188:107–20.

[17] Haase P, Thomas B. Test and optimization of a control algorithm for demand-oriented operation of CHP units using hardware-in-the-loop. Appl Energy 2021;294:116974.

[18] Ceglia F, Marrasso E, Roselli C, Sasso M, Tzscheutschler P. Exergetic and exergoeconomic analysis of an experimental ground source heat pump system coupled with a thermal storage based on hardware in loop. Appl Therm Eng 2022;212:118559.

[19] Calfa C, Yang Z, Li Y, Chen Z, O'Neill Z, Wen J. Performance assessment of a real water source heat pump within a hardware-in-the-loop (HIL) testing environment. Sci Technol the Built Environ 2023;29(10):1011–26.

[20] Rae C, Bhagavathy S, Thorpe B. Assessing the demand flexibility of storage-integrated heat pumps: A heating hardware-in-the-loop approach. In: 2025 IEEE PES innovative smart grid technologies conference europe (ISGT europe). IEEE; 2025, p. 1–5.

[21] Zinsmeister D, Lickleder T, Adldinger S, Christange F, Tzscheutschler P, Hamacher T, Perić VS. A prosumer-based sector-coupled district heating and cooling laboratory architecture. Smart Energy 2023;9:100095.

[22] Angelidis O, Zinsmeister D, Ioannou A, Friedrich D, Thomson A, Ganslmeier U, Falcone G. Development and experimental validation of a hydraulic design and control philosophies for 5th generation district heating and cooling networks. Energy 2024;308:132835.

[23] Sdringola P, Pipiciello M, Ricci M, Gianaroli F, Menegon D, Trentin F, Turrin F, Di Pietra B. Prosumers and district heating: Experimental validation of strategies to improve thermal energy production and consumption. Energy Build 2025;338:115713.

[24] Gissing SBTLJ, Eckstein PJL, Küfen J. Hardware-in-the-loop (HIL) simulation with modelica-a design tool for thermal management systems. Proc 10th Int Model 2014.

[25] Gross-Weege C, Lichius T, Baltzer S, Abel D. Control design for a thermal hardware-in-the-loop test bench for automobile thermal management systems. IFAC-PapersOnLine 2015;48(15):441–7.

[26] Mehrfeld P, Nürenberg M, Knorr M, Schinke L, Beyer M, Grimm M, Lauster M, Müller D, Seifert J, Stergiaropoulos K. Dynamic evaluations of heat pump and micro combined heat and power systems using the hardware-in-the-loop approach. J Build Eng 2020;28:101032.

[27] Chhugani B, Kirchner M, Littwin M, Lampe C, Giovannetti F, Pärisch P. Investigation of photovoltaic-thermal (PVT) collector for direct coupling with heat pumps: Hardware in the loop (HiL) and trnsys simulations. In: BauSim conference 2020, vol. 8, IBPSA-Germany and Austria; 2020, p. 120–7.

[28] Conti P, Bartoli C, Franco A, Testi D. Experimental analysis of an air heat pump for heating service using a "hardware-in-the-loop" system. Energies 2020;13(17):4498.

[29] Langerova E, Zavrel V, Matuska T. Hardware-in-the-loop testbed for evaluating heat pump energy flexibility control strategies: Design, evaluation, and experiment. Appl Therm Eng 2025;265:125595.

[30] Franco A, Bartoli C, Conti P, Testi D. Optimal operation of low-capacity heat pump systems for residential buildings through thermal energy storage. Sustainability 2021;13(13):7200.

[31] Renté N, Meljac L, Cauret O, Attonaty K, Tran CT, Stabat P. Design and validation of a heat pump digital twin and its control strategy towards the development of flexibility focused controllers. In: 8th international high performance buildings conference at purdue, July 15 – 18. 2024.

[32] De Carne G, Lauss G, D'Arco S, Srdic S, Wiegel F, Buticchi G, Kotsampopoulos P, Ashrafidehkordi F, Wald F, Schoder K, et al. Power hardware-in-the-loop for electrical systems: from research experience to guidelines for industrial testing. IEEE Open J Power Electron 2026.

[33] Holman JP, Gajda WJ. Experimental methods for engineers. McGraw-Hill; 2001.